Article:
Hayes, S., Fletcher, D. orcid.org/0000-0002-1562-4655, Beagles, A. et al. (1 more author) (2020) Effect of contact wire gradient on the dynamic performance of the catenary pantograph system. Vehicle System Dynamics. ISSN 0042-3114

https://doi.org/10.1080/00423114.2020.1798473

Taylor & Francis
Taylor & Francis Group

Vehicle System Dynamics
International Journal of Vehicle Mechanics and Mobility

ISSN: (Print) (Online) Journal homepage: https://www.tandfonline.com/loi/nvsd20

Effect of contact wire gradient on the dynamic performance of the catenary pantograph system

Sam Hayes , David I. Fletcher , Adam E. Beagles & Katherine Chan

To cite this article: Sam Hayes , David I. Fletcher , Adam E. Beagles & Katherine Chan (2020): Effect of contact wire gradient on the dynamic performance of the catenary pantograph system, Vehicle System Dynamics, DOI: 10.1080/00423114.2020.1798473

To link to this article: https://doi.org/10.1080/00423114.2020.1798473

Published online: 30 Jul 2020.

VEHICLE SYSTEM DYNAMICS
https://doi.org/10.1080/00423114.2020.1798473

Effect of contact wire gradient on the dynamic performance of the catenary pantograph system

Sam Hayes [a], David I. Fletcher[a], Adam E. Beagles[a] and Katherine Chan[b]

[a]Department of Mechanical Engineering, University of Sheffield, Sheffield, UK; [b]Furrer+Frey GB Ltd, London, UK

ABSTRACT

This paper considers the interaction between a train mounted pantograph and a railway overhead line, presenting results that could be used to reduce the cost of installing overhead electrification, for example, by reducing the need for expensive bridge reconstruction. Ideally, overhead wires would run at a constant height parallel to the track, however, gradients are often unavoidable due to clearance limitations requiring lower wire heights at bridges and tunnels, and higher heights above level crossings. In this study, the influence of a range of contact wire gradients on the contact force between the overhead line and pantograph has been studied using a validated finite element model. Introducing a windowing technique to identify discrete dynamic behaviours found that overhead wire gradients can be increased with minimal effect on the contact force, showing current wire gradient limits are conservative. This may open up opportunities for electrification, less disruptive than following current standards.

ARTICLE HISTORY
Received 22 November 2019
Revised 16 June 2020
Accepted 2 July 2020

KEYWORDS
Electrification; railway infrastructure; dynamics; overhead line equipment; catenary/pantograph interaction; wire gradients

Notation

C	Constant
$F_{D\max}$	Discrete maximum
$F_{D\min}$	Discrete minimum
F_m	Arithmetic mean of contact force
$F_{S\max}$	Statistical maximum ($F_m + 3\sigma$)
$F_{S\min}$	Statistical minimum ($F_m - 3\sigma$)
T_{con}	Contact wire tension
T_{mes}	Messenger wire tension
c_i	Damping factor of the i^{th} damper
g	Gravitational acceleration
k_i	Stiffness constant of the i^{th} spring
m	Mass per unit length
m_{con}	Contact wire mass per unit length
m_i	i^{th} mass

CONTACT Sam Hayes shayes2@sheffield.ac.uk

m_{mes}	Messenger wire mass per unit length
x_0	Midspan offset
x	Longitudinal direction along wire horizontal profile
y	Vertical direction along wire vertical profile
z	Lateral direction across the track
α	Mass proportional damping factor
β	Stiffness proportional damping factor
σ	Standard deviation of contact force

Introduction

With an ever-increasing desire for reduced journey times, higher capacity and less environmental impact, electrification is now the standard for high speed train operation. In the UK, approximately 40% of the network is electrified (two-thirds 25 kV AC OLE and one-third, third-rail DC), accounting for almost 50% of train miles covered [1].

The smooth interaction between trains' pantographs and overhead electric contact wires is important to the reliable running of an electrified rail network. The dynamic behaviour of sliding contact between a level railway contact wire and a train pantograph has been extensively studied in recent years [2–4]. Here, 'level' is used to indicate that the distance from the rail track to the support locations of the contact wire is constant. However, there are fewer investigations of the influence of gradients in the contact wire on this interaction where support height varies.

To add overhead line equipment (OLE) to a railway line with pre-existing features such as bridges, tunnels, level crossings, and stations the height of the overhead contact wire is often forced to vary through the existing infrastructure in contrast to track purpose built with sufficient clearances. Left unchanged, these elements of infrastructure would need to be moved, would have a potential for increased arc discharge events to structures, or would need to be rebuilt at high cost. The wire gradients permitted on the UK rail network are described by BS EN 50119:2009 [5], including maximum gradients that depend on the railway line speed (e.g. maximum 1:500 for speeds between 200 and 250 km/h). This gradient becomes difficult or impossible to achieve when low wire height locations of 4.5 m are situated close to level crossings or stations for which wire heights typically greater than 5.6 m are required [6]. This situation is prevalent in the UK where bridges are close to level crossings and stations. Figure 1 shows a possible geometry arrangement where a level crossing and bridge could be too close together to allow for the required gradients.

For level contact wires (zero gradient), good contact between the pantograph and contact wire is required to ensure good current collection and minimise contact loss, which would result in arcing between the contact surfaces. Sliding contact between the pantograph carbon and the contact wire induces mechanical wear on the contact wire that can be approximated by the Archard wear equation [7]. More comprehensively the contributions of both mechanical and electrical wear are described by the model of Bucca and Collina [8]. Damage caused by melting and vaporisation of the contact wire [9] and pantograph due to thermal effects, promotes additional wear [10] further limiting the service life.

Previous analyses of the interaction between the pantograph and contact wire have focused on level wires [11–13] installed on straight track, such as the arrangement shown

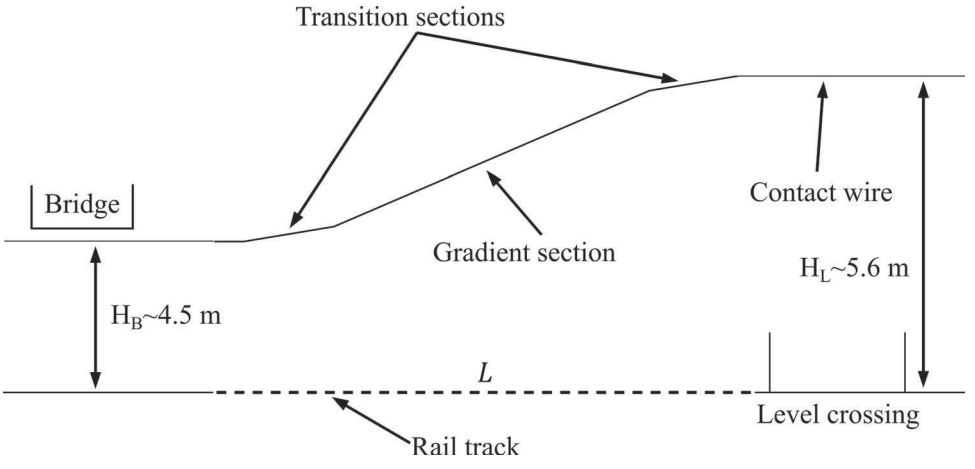

Figure 1. Side view of a wire geometry when a level crossing and bridge are separated by a distance L. The masts, droppers, and messenger wire that support the contact wire are omitted for clarity.

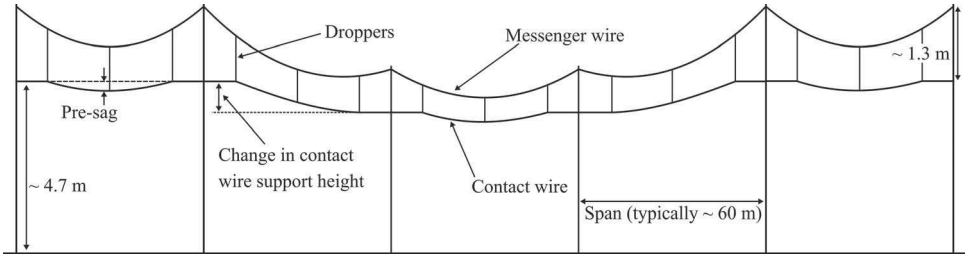

Figure 2. Typical overhead line equipment (OLE) represented as a 2D schematic. The contact wire is suspended from the catenary wire by droppers and the overhead equipment is supported by masts positioned beside the track. Dimensions represent typical UK arrangements with wire gradient defined by the change in the contact wire support height divided by the span length.

in the left-most span of Figure 2, whilst the influence of curved track on the catenary pantograph interaction was investigated by Antunes et al. [14]. A level wire arrangement such as shown in Figure 2 is typical for a range of 'simply sagged' systems or 'presagged' systems around the world, that is those with a defined sag between the first and last dropper to compensate for the reduced vertical stiffness at mid-span. A range of models predicting their behaviour have been validated according to BS EN 50318 [15] with many covered in a benchmark by Bruni et al [16], however, none present a model with wire height changes such as the one shown in Figure 2.

Nåvik and Rønnquist sought to increase the train running speed of an existing electrified line in Norway [17] and noted that increased wire gradients resulted in increased wire uplifts at the supports. The Nordic system uses a contact wire tension of 10 kN, lower than the 16.5 kN wire tension applied to the UK Series 1 system studied in this paper. The models of Nåvik and Rønnquist included a wire height decrease but no increase and thus don't predict dynamic response to an increasing wire height. Naturally, both increasing and

decreasing wire heights are expected in the approach and passage of a low-height overbridge. The work of Nåvik and Rønnquist utilised a two-mass pantograph approach with train running speeds up to 200 kph, the work presented here utilises a three-mass approach with speeds between 130 and 225 kph.

Calculating contact loads during height transitions allows for better prediction of the sliding contact wear regime during train operation. The model presented here allows for prediction of loads and contact loss and can assist in determining preventative steps to maintain the life of the overhead line.

In this paper, a finite element model of a system undergoing wire height changes is presented to investigate the influence of increasing steepness of wire gradient on the interaction between the catenary and pantograph. Section 2 presents the modelling methodology and the gradient cases considered in this work. Validation of the new height-change model is presented in Section 3 using test track data, whilst the simulation results and discussions are in Section 4. Final conclusions based on the results are given in Section 5.

Modelling methodology

This work extends the method developed by Beagles et al. [18], using a finite element representation of the wire geometries. Four geometries were used during this study and Figures 3–6 show the geometries created during the modelling process of the four models used throughout this paper, shown vertically exaggerated and horizontally compressed. In each of the figures, 1 m vertically corresponds to 120 m horizontally. The four models used are:

1. Model 1: the test track OLE used in the validation case
2. Model 2: reducing contact wire height over a range of gradients whilst maintaining the system height (i.e. the dropper lengths)
3. Model 3: both the contact wire and system heights reducing
4. Model 4: the contact wire height maintained but reduced the system height.

In models 3 and 4, in the central spans the droppers are approximately 50% shorter when compared with model 2.

Each of these models is relevant to a particular real-world installation. Here, using model 2, the influence of the gradients described in Table 2 are determined. Model 3 is used to investigate the influence of altered dropper lengths changing both the height of the

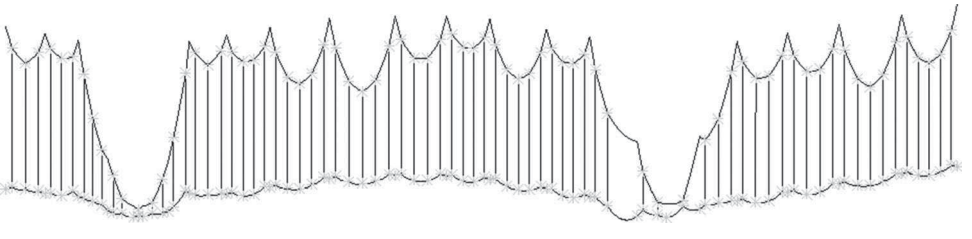

Figure 3. Model 1 is a representation of the real overhead line geometry installed at Network Rail's Melton Rail Innovation and Development Centre, used in the validation case.

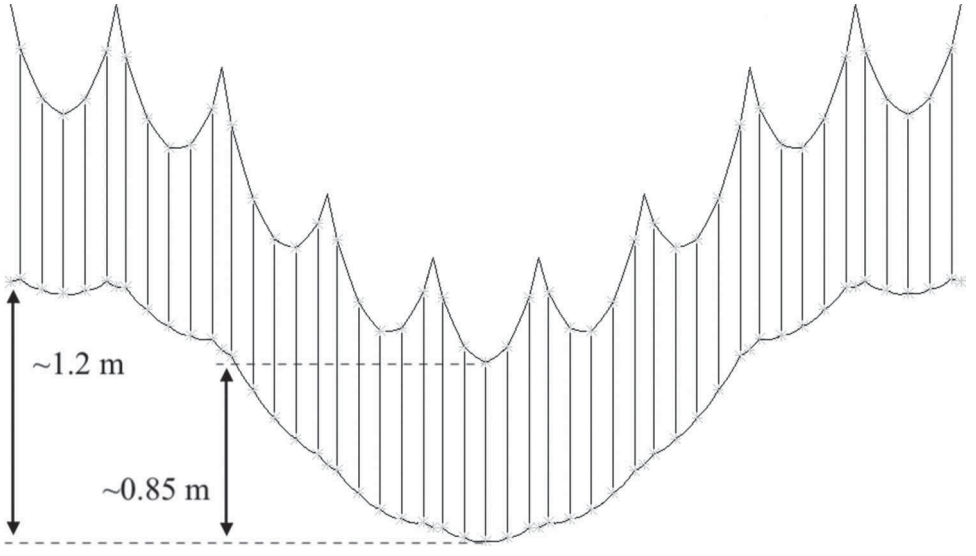

Figure 4. Model 2 used to investigate the influence of a range of contact wire gradients on the catenary-pantograph interaction. Shown is the case of a 1:100 wire gradient and the length of the droppers in each span was maintained thus leaving the system height unchanged.

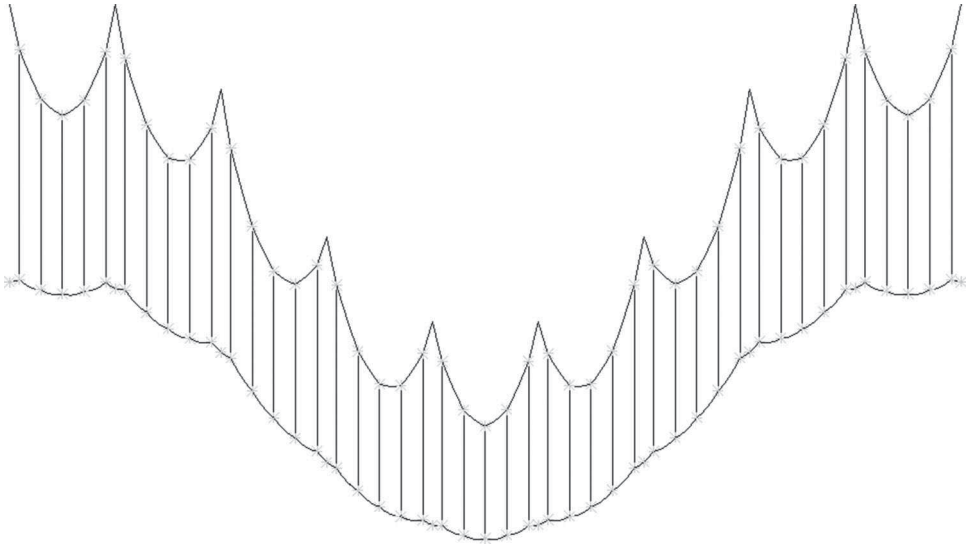

Figure 5. Model 3 allowing for a change in the system height as well as a reduction in the contact wire height. The reduction in the system height is highlighted.

contact wire and the system height, representing a more realistic OLE installation through a low clearance structure and model 4 represents a system with no change in the contact wire gradient and only a reduced system height.

Validation of the graded overhead line (model 1) was performed using data provided by track tests using a British Rail Class 395 high speed electric multiple unit at Network Rail's

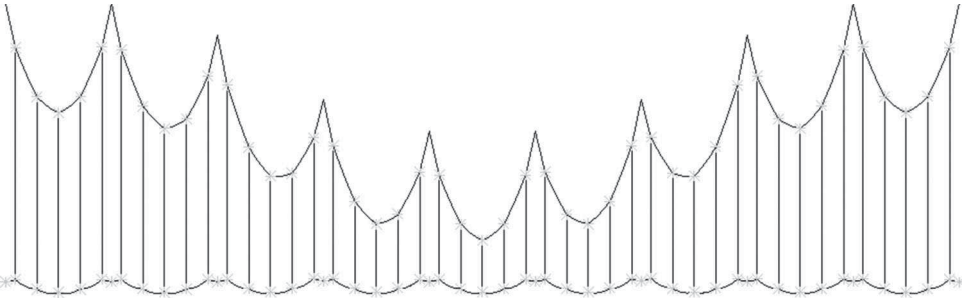

Figure 6. Model 4, showing a system with a reduced system height only.

Melton Rail Innovation and Development Centre (RIDC) [19,20]. The modelling process was divided into five steps, details of which are provided in the following sections:

Step 1 Creation of OLE geometry,
Step 2 Determination of static wire equilibrium,
Step 3 Settling step,
Step 4 Introduction of pantograph model and dynamic simulation, and
Step 5 Post-processing.

Step 1 Determining the shape of the catenary

For model 1, the geometry was provided by Network Rail as part of a series of tests investigating overhead line faults and allowed for an 'as-fitted' representation of the OLE to be created. The shape of the messenger wire for all geometries was approximated by using the catenary curve,

$$y(x) = \frac{T_{\text{mes}}}{mg} \cosh\left(\frac{mg}{T_{\text{mes}}}(x - x_0)\right) + C \tag{1}$$

where the height $y(x)$ at location x along the wire is a function of the tension of the messenger wire, T_{mes}, and the total mass supported (contact plus messenger wires) per unit length, m. The constant C was uniquely determined by the wire heights at the support structures which were taken to be fixed, and x_0 is the offset of the midspan when the support heights differ between the ends of the span. The length of the droppers for the idealised geometry were chosen to achieve a presag of 60 mm, that is 1000th of the span length 60 m, based on the shape of the catenary wire as calculated by Equation (1). Whilst Equation (1) gives the curvature for an unloaded catenary this is an approximation to the true geometry of the installed catenary as the addition of droppers and non-uniform load distorts the initial catenary shape.

For models 2, 3, and 4, each span was 60 m long and the contact wire was suspended from the catenary wire using five droppers. The locations of the droppers within each span and their lengths used in model 2 are given in Table 1.

Gradients

For model 2 the wire gradient was increased through the range of values shown in Table 2. Transitions between any wire gradients were taken to be half that of the desired gradient,

Table 1. Dropper locations and their lengths used in model 2.

Dropper	1	2	3	4	5
Location from start of span (m)	5.5	17.75	30	42.25	54.5
Length (m)	1.09	0.904	0.845	0.904	1.09

Note: Dropper lengths chosen to match those in a 60 m span from the validation case in Beagles et al.

Table 2. Maximum gradient, number of spans, total wire length, and working section ends used for model 2. The working section begins at 300 m in each case.

Maximum gradient	Number of spans at maximum positive gradient	Number of spans at maximum negative gradient	Number of spans used in simulation	Total length of wire run (km)	Working section end (m)
1:500	9	9	46	2.76	1800
1:400	7	7	40	2.40	1560
1:300	5	5	34	2.04	1320
1:200	3	3	28	1.68	1080
1:100	1	1	22	1.32	840

e.g. a transition span between a level wire and a 1:500 graded wire was 1:1000. In each simulation, there were a total of four transition spans (two when the wire was going down and two going up).

Beagles et al. followed BS EN 50318:2002, which specifies that a minimum of ten spans of the reference model are to be simulated with data taken from the central two spans only to account for any boundary effects and approximately 675 m of OLE were used in the test track validation case. To transition between wire heights and return to the original height, it was necessary to extend the number of spans in the model so that end effects were kept out of the working section of the model. The length of the model, which occupied up to 46 spans, along with the length of the working sections are shown in Table 2. No overlap sections were included in the modelled geometries to remove unwanted dynamic effects due to discrete OLE elements. By removing these discrete features, the core gradient effects are highlighted. Figure 7 shows the working section used for the 1:100 wire gradient case. Each of the other gradient cases have similar wire geometries but extended over more spans, corresponding to the distance for the wire to fall or rise at each gradient considered.

Step 2 Static wire equilibrium and imposition of the boundary conditions

An initial static load step was used to determine the wire equilibrium after gravitational acceleration, and longitudinal tensions were applied to the OLE components, creating the desired geometry.

Global boundary conditions were applied to the wire geometry in Step 2, constraining the wire geometry against any lateral (z direction) deflections and rotations about the longitudinal (x direction) or vertical (y direction) axes, a configuration found to avoid numerical convergence issues. The catenary and contact wires were also constrained at the first support in the x direction but not at later supports, allowing for vibrations in the wire to transmit freely between spans. Wire tension of 13 and 16.5 kN was applied to the messenger and contact wires respectively. The maximum design speed for the given contact wire tension was 320 km/h. Lateral inertia at the support locations was provided by registration arms represented by point mass additions applied at the nodes corresponding

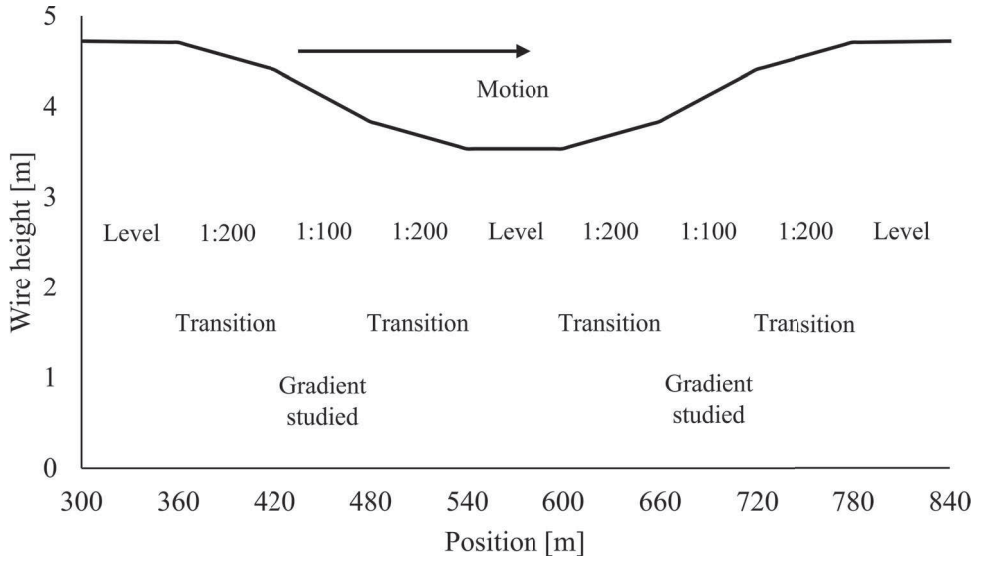

Figure 7. The contact wire height in the working section of the OLE when the gradient is 1:100. Masts are located every 60 m, highlighted by the vertical lines. The contact wire gradient in each span is given (Level, 1:200, etc). Sharp transitions between spans are exaggerated by the ratio of 120:1 between horizontal and vertical scales and were not present in reality.

to the registration arm locations. The point mass additions to the wire geometry for the registration arms and contact and messenger wire clamps are 0.924 and 0.15 kg respectively. Details of the element types used can be found in Beagles et al. [18].

Step 3 Settling step

This step was used to allow for the damping of accelerations caused during the formation of the desired wire geometry. This was achieved using a load step with transient effects turned off and resulted in a wire in static equilibrium.

Step 4 Simulation of contact between pantograph and OLE

Once the OLE geometry has been created, the pantograph model was introduced and brought into contact with the OLE. A dynamic simulation of the contact between them was performed; as described below.

Pantograph model

A three-mass pantograph model representing a Brecknell Willis HSX pantograph was used with parameters determined experimentally by Conway [21] using a pantograph test rig at DB Systemtechnik, Munich. The parameters and the pantograph model used are shown in Table 3 and Figure 8 respectively. The parameter values given are experimentally derived and as such don't correspond directly to individual elements of the pantograph, they could be distributed and optimised in different ways to achieve similar dynamic performance [11,22]. To achieve a tractable model, not every component of the pantograph can be captured in detail. Since the static uplift at the contact wire is required to be independent of the operating height of the pantograph as in BS EN 50206-1 [23], a null spring stiffness between the train and the lower mass was given. Damping within the system ensures it is

Table 3. Parameter values used for lumped mass representation of the pantograph. Values from [21].

Mass (kg)	Damping (Ns/m)	Stiffness (kN/m)
$m_1 = 3.53$	$c_1 = 32.6$	$k_1 = 0$
$m_2 = 7.5$	$c_2 = 0$	$k_2 = 5$
$m_3 = 5.3$	$c_3 = 70$	$k_3 = 6.3$

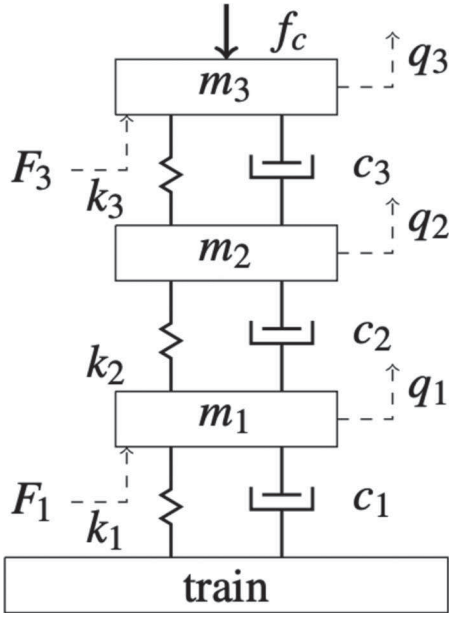

Figure 8. Three degrees of freedom mass-spring representation of a pantograph adapted from [18]. The force F1 is the static uplift force taken to be 70 N, and aerodynamic force F3 N in this case is given by 0.01031v2 N, where v is the train speed.

still capable of reflecting force variation with change of height during the dynamic simulation. Motion of the pantograph due to vertical train movement on the suspension was not considered in this model and the bottom of the pantograph was fixed in the vertical direction relative to the other components. All pantograph components were constrained against lateral displacement.

Surface to surface contact utilising 3D line-to-line contact elements overlaid onto the pantograph collector strip and contact wire during the solution process allow for dynamic separation of the pantograph and OLE. The penalty method utilised in [18] between the two contact elements was maintained here. Contact is detected when the two contact elements penetrate, and the contact force is determined using the contact gap size and the penalty stiffness of 50 kN.

Dynamic simulation of contact

Step 4 uses the settled geometry generated by Step 3 to perform a transient analysis with the pantograph moving at a speed of 200 km/h. A fixed time step was determined by the

frequency of data collection. In this study the frequency was 200 Hz, matching the test track data collection frequency and ten times the frequency of interest of 20 Hz required by BS EN 50318, giving a time step of 0.005 s. For the given frequency and speed, the pantograph moves 0.278 m with each time step, less than the mesh element size of 0.5 m.

Damping of the overhead line is applied globally using Rayleigh damping. The mass and stiffness proportional damping factors are $\alpha = 0.0055/s$ and $\beta = 0.011$ s respectively [18].

Step 5 Post processing and generation of outputs

Outputs generated by the model are focused on the displacement of the nodes describing the pantograph head and the contact wire. At each time step, the displacement of these nodes and the contact stiffness was recorded. The output for a level contact wire is provided in [18] where the model was found to be in good agreement with both the reference model and test track data.

Due to the use of point masses at nodes describing the location of the registration arms, calculation of the support uplift is also possible.

Post-processing of the data in the validation case was performed in MATLAB with data filtered using a 20 Hz low-pass filter. The sixth order filter, as required by BS EN 50317:2012 [24], attenuates data with a frequency greater than 20 Hz and returns the force data in the time domain. Removing this attenuation by filtering with a cut off of up to 80 Hz, indicated the presence of higher peak forces at higher frequencies, as would be expected [25] and this is explored in the results below.

Validation of height transition OLE model with real line data

Validation of the model was performed using measured data from Network Rail's Rail Innovation and Development Centre (RIDC) at Melton, UK generated using a Hitachi Javelin (Class 395) train. For the validation, a section of real installed OLE geometry including two low clearance overbridges was chosen corresponding to approximately 900 m of OLE. Figure 3 shows model 1, the representation of the wire geometry at the RIDC test track.

Table 4 gives the results for the forces predicted by the model as well as the ±20% band allowable in BS EN 50318:2002 [15] to account for variation in the real-world data not captured by the model of the real geometry, such as weather effects, damage to the OLE or deviations in the track. The results obtained by simulations are in good agreement with those from the test track.

All modelling results fell within the ±20% band of allowable deviation from the measured real-world data. The greatest difference was peak contact force with a difference of 14.3%. These large peaks in contact force were predicted by the model at locations where the pantograph moved from an upward-sloping section into an ungraded span.

The higher contact force in the simulated results reflects the acceleration required to change the pantograph direction due to the change in the wire gradient. The simulated mean contact force varies from the test track data by only 2 N representing very good agreement and there was no contact loss for either measured or simulated data.

Comparison was made between the test track data and the contact force versus position modelling predictions. The considerable variation in the span lengths (between 9 and 65 m) disrupted the repetitive pattern which might otherwise have existed for a more uniform installation. The peak force locations coincident with supports were correctly predicted,

Table 4. Model results for the test track and model predictions for the entire OLE length.

Statistical parameter	Measured contact force −20%	Measured contact force	Simulated contact force	Measured contact force +20%
F_m	82.5	103	105	124
σ	19.6	24.5	27.0	29.4
F_{Dmax}	140	175	200	210
F_{Dmin}	23.9	29.8	29.2	35.8
F_{Smax}	141	177	186	212
F_{Smin}	23.8	29.8	24.3	35.7

Notes: All force and standard deviation values in N. See notation for definitions of statistical terms.

however, some deviation between the measured and simulated data occurred as not every detail of the overhead line system could be modelled. For example, wear state of the contact wire was not included. The relatively large acceptance band of ±20% in BS EN 50318 exists because a computationally tractable cannot include every detail of a real-world installation.

The statistical output provided in Table 4 also provides evidence that the use of a three-lumped mass model of the Brecknell Willis HSX pantograph is suitable for the modelling of large-scale height changes, which are explored in the next section.

Results and discussion

In this section, the results of runs using models 2, 3 and 4 are presented. Because the analyses included gradient variation throughout the site, analysis was performed: (1) using the whole site as expected in EN 50318; and (2) using a moving window analysis to focus on the discrete behaviours across individual parts of the site such as transition regions.

Varying the contact wire height and maintaining the system height

Data generated by simulation of the interaction between the pantograph and contact wire is presented in Table 5. Each column details the output as required by BS EN 50318:2002 [15] for wire gradients ranging from 1:500 up to 1:100.

Overall behaviour of the catenary/pantograph interaction

From Table 5, increasing the wire gradient has little effect on the overall performance of the interaction demonstrated by the 0.3% change in the mean contact force between the wire gradients of 1:100 and 1:500. There is a 40% increase in the standard deviation of the contact force which can be traced to the peaks in contact force shown in Figure 9 being

Table 5. Results for model 2 for each gradient.

Statistical parameter	Level	1:500	1:400	1:300	1:200	1:100
F_m	112	112	112	112	112	112
σ	11.5	12.9	13.0	13.6	14.7	18.0
F_{Dmax}	154	161	162	164	170	184
F_{Dmin}	90.2	86.4	85.5	83.6	80.1	75.4
F_{Smax}	146	151	151	152	156	165
F_{Smin}	77.4	72.9	72.6	70.9	67.5	57.3

Notes: Mean and standard deviation are taken over the working section described earlier. The data includes variation in the contact force due to both decreasing and increasing wire heights. All results are given in N.

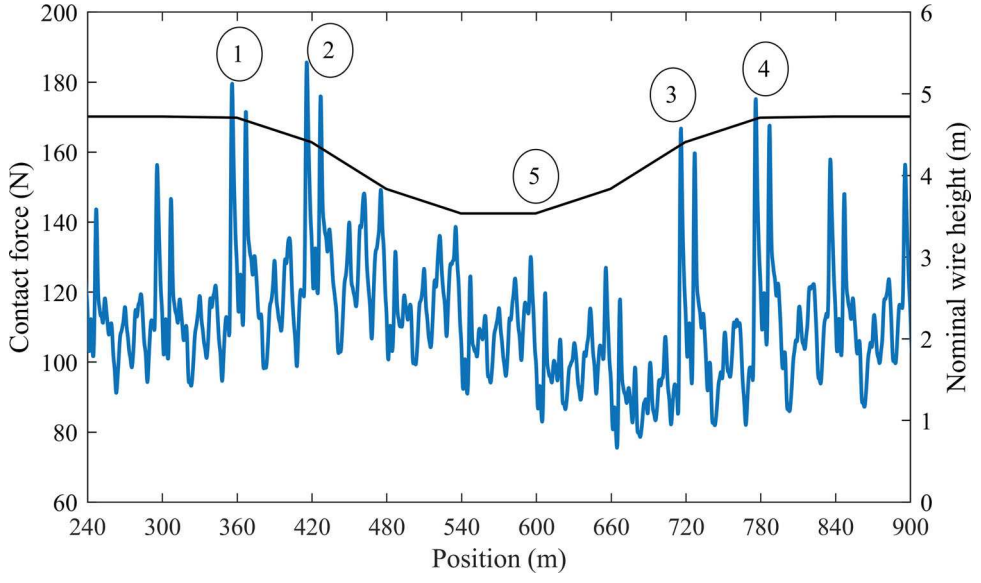

Figure 9. Force trace for a wire gradient of 1:100 for model 2. The corresponding contact wire geometry is indicated by the solid line and mast locations are given on the horizontal axis. Key locations referred to in the text are numbered 1 - 5, and the nominal contact wire height is between 3.5 and 4.7 m.

predicted to occur when there is a change in the wire gradient. Increasing the gradient to 1:100 increased the peak contact force by 22%. There was a consistently increasing maximum contact force (the mean has remained almost constant in each of the considered gradients) at discrete locations of OLE for increasing gradients between 1:500 and 1:100. A similarly consistent trend in minimum contact force can be observed, with lower minima predicted for the steeper gradient cases. These are consistent with the larger standard variation.

As identified in the validation stage, the peak contact force is predicted when the pantograph accelerates vertically due to a change in the wire gradient. For example, at location 1 indicated in Figure 9, the wire gradient changes from level to 1:200 and a contact force peak of 179 N occurs. Similarly, as the gradient changes from 1:200–1:100 at location 2, a force peak of 187 N occurs. This is consistent with accelerating the pantograph downwards due to the change in the wire slope. As the pantograph moves along the wire through the height transition, a further peak in force occurs at location 3 when the gradient changes from 1:100 to 1:200 and the pantograph transitions towards the ungraded wire. This further acceleration results in a peak force of 162 N followed by a peak of 171 N when the gradient changes from 1:200 to level at location 4.

Table 5 gives the statistical values when the model output is filtered at 20 Hz. The data was also filtered up to 80 Hz. Figure 10 shows the statistical output for each of the gradients considered using model 2. In Figure 10(b), it can be seen that the peak forces rise as higher frequencies are kept during the filtering process. In the case of a wire gradient of 1:100, the peak force when the data was filtered at 50 and 60 Hz, was 199 N compared with 186 N when filtering at 20 Hz. The increase in contact force was similar in magnitude in all the considered cases of around 7%.

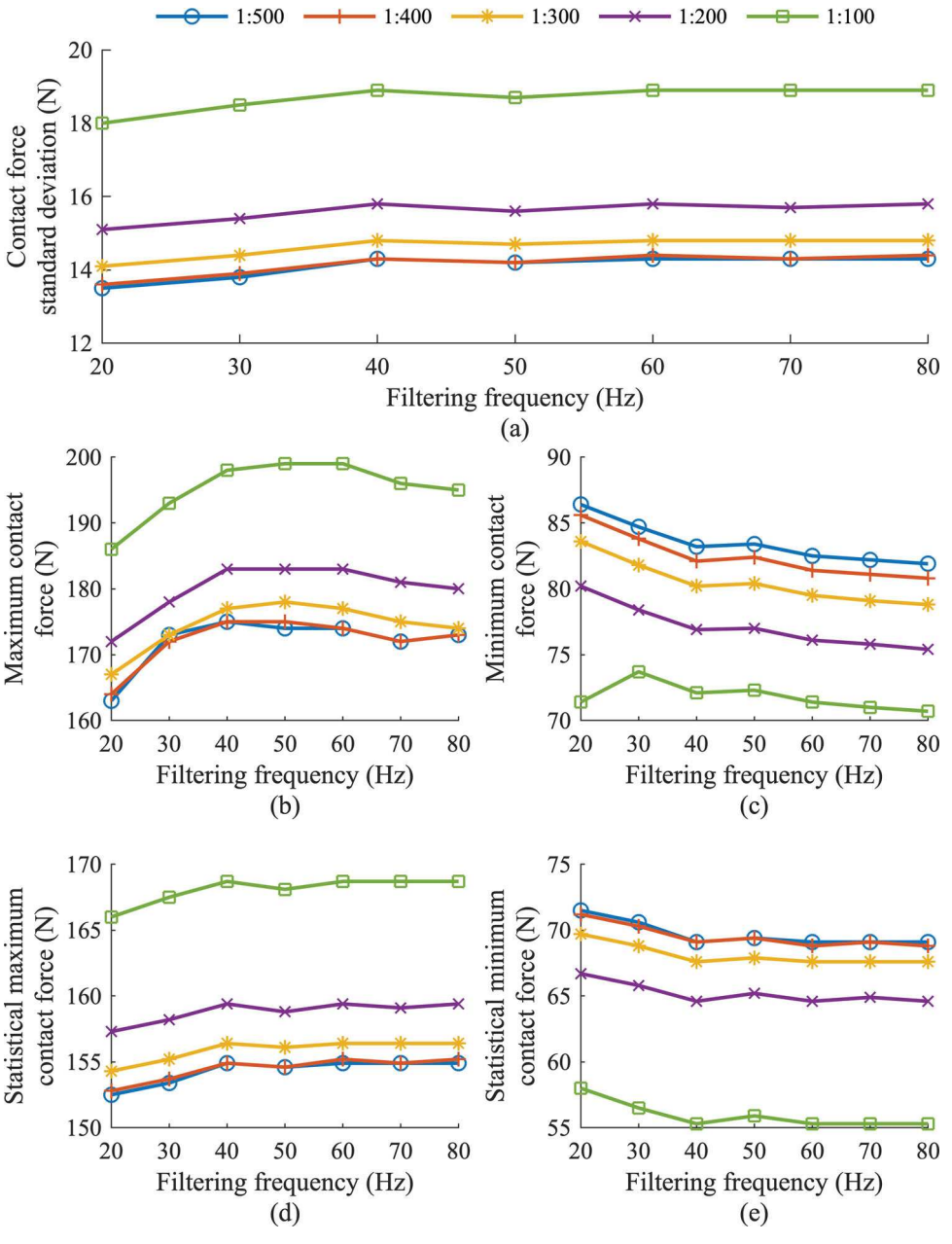

Figure 10. Variation in the statistical parameters after filtering the modelling output. Legend indicates the gradient considered in each case.

Minimum contact force also shows a similar trend with increasing filtering frequency as shown in Figure 10(c). As the filtering frequency increased, the minimum contact force typically decreased by around 5 N. The variation in the statistical maxima and minima was driven only by the variation in the standard deviation as the mean was unchanged with respect to filtering frequency.

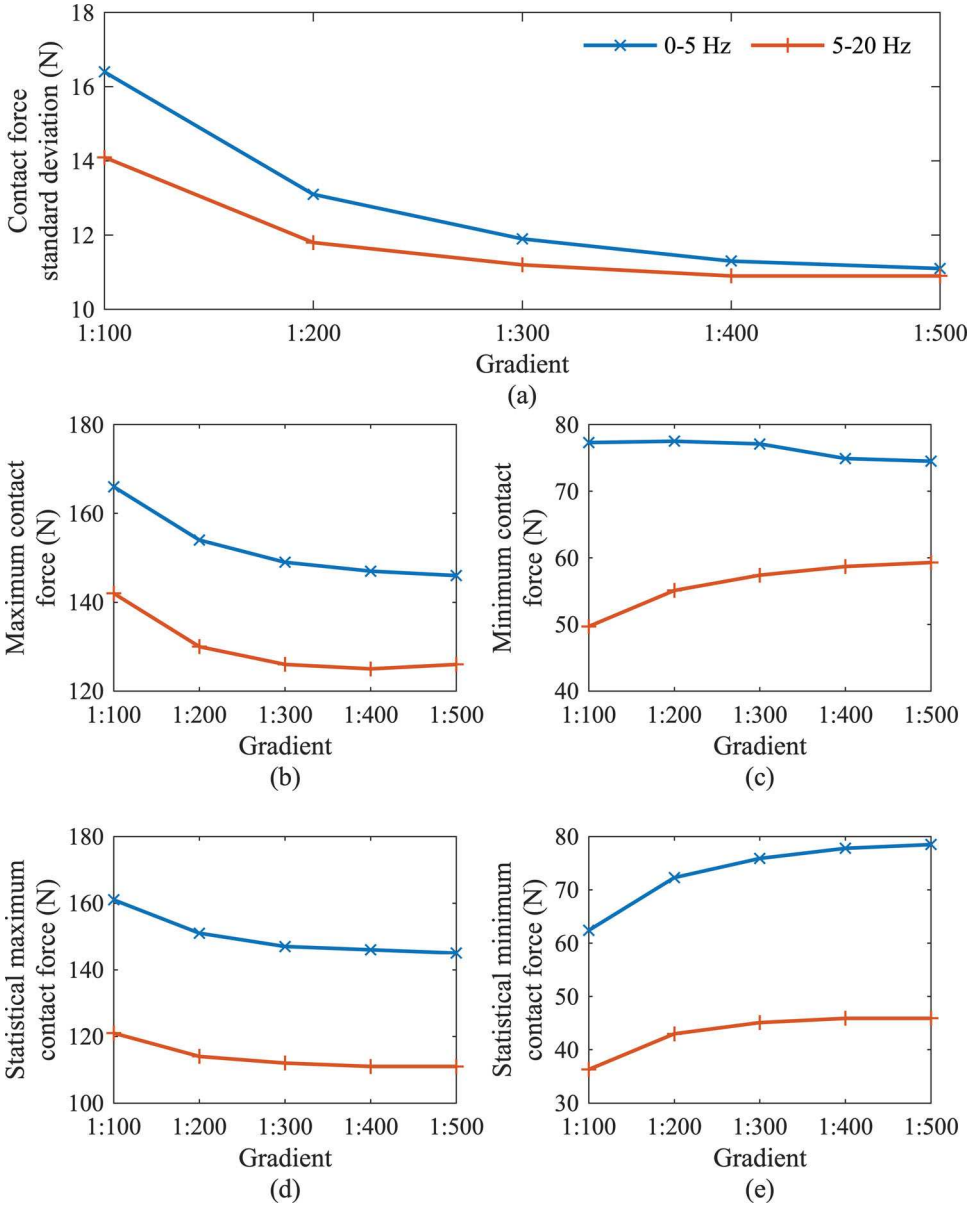

Figure 11. Statistical output for below 20 Hz frequencies. A low pass filter of 5 Hz and a band pass filter of 5–20 Hz was applied in each case. Legend indicates each frequency band.

The statistical output of the model below 20 Hz is given in Figure 11. It can be seen that the low frequency behaviour in the 0–5 Hz range such as the dropper passing frequency (4.89 Hz) is the dominant component of the peak contact force, with the contact force peak around 20 N larger in the 0–5 Hz range when compared with the 5–20 Hz range. As in Table 5, standard deviation increases with increasing steepness of wire gradient and the low frequency behaviour causes a larger variation in the contact force with steeper gradient,

whereas the variation due to different frequency behaviour is of similar magnitude when the contact wire gradient is shallow.

From the histogram of forces in Figure 12, with increasing wire gradient, the contact force between the pantograph and contact wire is spread across the range of forces consistent with the increased standard deviation. With increasing steepness of gradient, excess of kurtosis decreased by 55% indicating that the predicted contact force for a steeper gradient, occurred more often at the extremes of the force distribution. This is consistent with the histogram showing a sharper decline in number of extreme force events when the gradient was 1:500 compared with 1:100. In all cases, there was no predicted contact loss and the maximum contact force for a gradient of 1:100 is 14% higher than the maximum at 1:500.

The increased occurrence of low contact force in the histogram in Figure 12 relates to the end of the downward wire run between locations 2 and 3 in Figure 9 and to location 5, when the wire begins to rise again. In these locations, the pantograph must accelerate upward to change direction and maintain wire contact but its rate of acceleration is set by the finite static and aerodynamic uplift forces and is therefore limited. An increased static uplift to counteract the reduced contact force while the wire height increases could be applied, but with a conventional passive pantograph, this would give an increased contact force across the entire system shortening the overall system life. An active pantograph with a variable uplift throughout the height transition would provide a means of achieving a contact force with lower variation.

The variation in the contact wire uplift at the supports near to the graded contact wire is also of interest when considering the influence of the gradient. The wire uplifts when the contact wire gradient is 1:500 and 1:100 are given in Figure 13. As with level wire, vertical oscillations are present in the contact wire as the pantograph arrives at the support, since

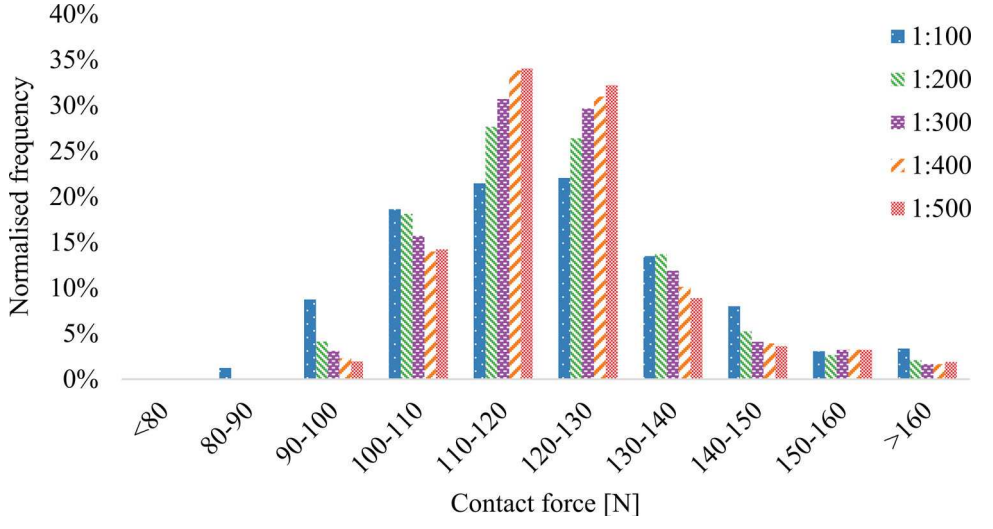

Figure 12. Histogram of contact force for each wire gradient for model 2. Normalised frequency indicates the percentage of data falling into each bin accounting for the number of data points in each simulation.

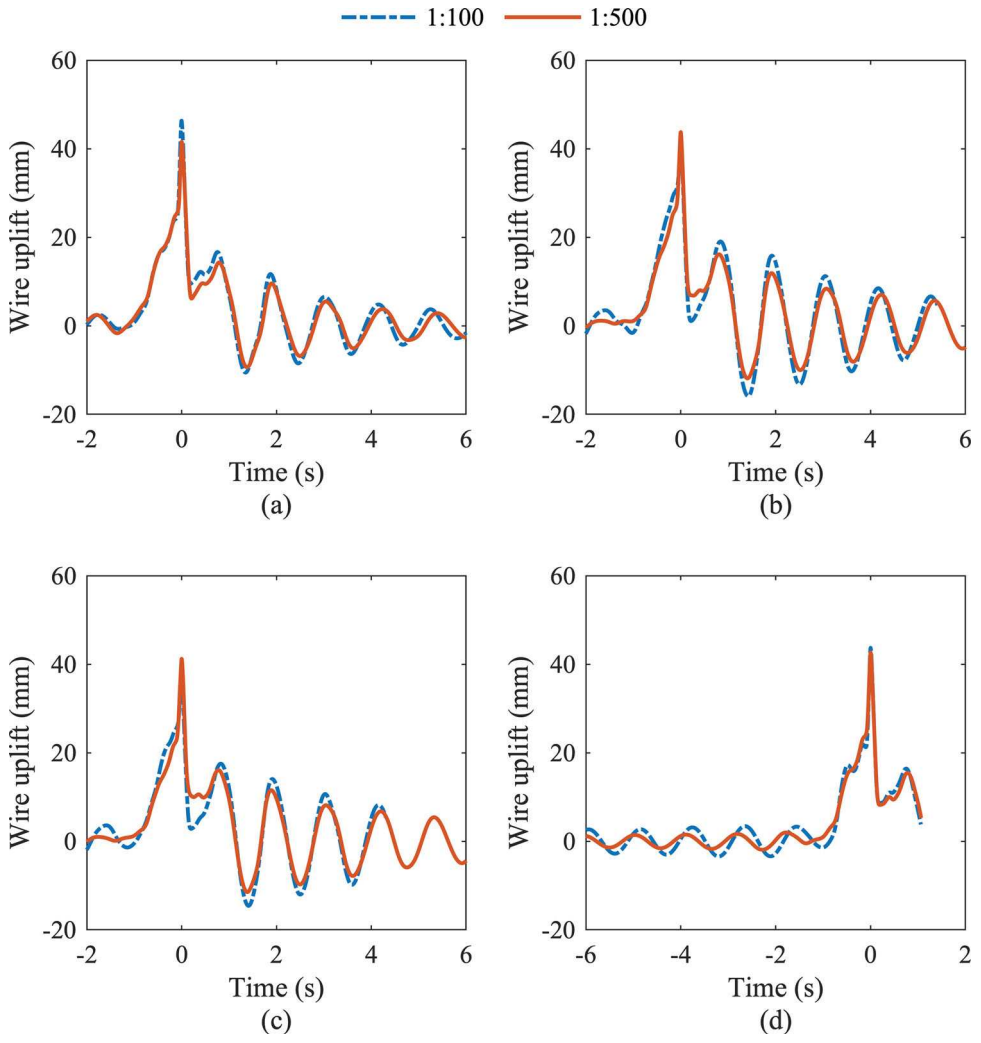

Figure 13. Wire uplift at supports at (a) the beginning of the first transition span, (b) the end of the second, (c) the beginning of the third and (d) the end of the fourth. Legend indicates the gradient being considered and zero time indicates the time the pantograph passing time.

the wave propagation speed, given by the square root of the ratio of contact wire tension and contact wire mass per unit length [26], is approximately 121 m/s, well ahead of the pantograph speed of approximately 56 m/s.

In both cases, the wire uplift at supports was around 40 mm and the largest variation was found at the beginning of the first transition span, where the uplift when the wire gradient was 1:100 was 12% larger than the uplift when the wire gradient was 1:500, shown in Figure 13(a). This increase in wire uplift was consistent with the 14% increase in peak contact force which was predicted in the first transition span from the level to decreasing wire height. The larger forces predicted due to a 1:100 wire gradient also led to an increase in the oscillation amplitude in the contact wire.

Analysis using a moving window

The previous section described the results of the catenary/pantograph interaction of model 2 across the whole of the working section. For a wire gradient of 1:500, this represented a working section length of 1800 m, however, discrete features may be hidden when taking averages of forces across this length. To overcome this, a moving window of length 60 m corresponding to a single span of 60 m was generated.

From Figure 14, it can be seen that the range of moving contact force as the analysis window traverses the downward to upward gradient contact wire sections is greatest for steep gradients and decreases as gradients become shallower. To account for the different length models, the horizontal distance required for each gradient is scaled so each section of the model corresponds to a unit length as follows:

Section 0–1 corresponds to the first ungraded span followed by the first transition,
Section 1–2 corresponds to the primary falling gradient spans,
Section 2–3 corresponds to the gradient transitions and central ungraded span
Section 3–4 corresponds to the primary rising gradient spans, and
Section 4–5 corresponds to the final gradient transition and ungraded span.

Table 6 summarises the variation in the magnitude of the average contact forces shown in Figure 14 and contact force standard deviation. The range of mean contact force between 1:500 and 1:100 increased by approximately 20 N. A larger range in the standard deviation of the contact force with an increasing gradient was also predicted, which is not unexpected when considered with the changes in the mean contact force. Unlike the changes in the

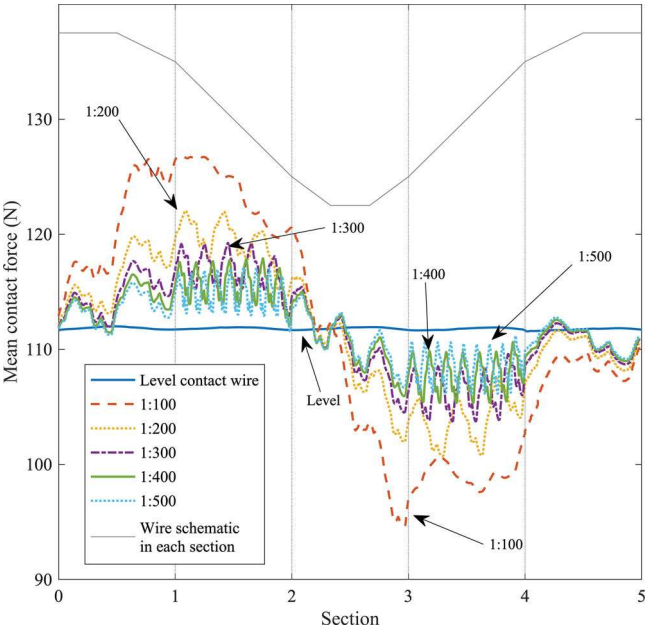

Figure 14. Mean of the contact force for model 2 for each gradient investigated using a 60 m moving window. Legend indicates the gradient used in each case.

Table 6. Variation in the magnitudes of the mean and standard deviation of the average contact force calculated using the moving window.

Gradient	Range of mean contact force	Range of force standard deviation
Level	0.437	0.660
1:500	10.9	3.0
1:400	12.6	5.0
1:300	15.5	4.9
1:200	21.3	6.6
1:100	32.2	10.3

Notes: Data are for increasing steepness of gradient in model 2 compared with the level case. Quantities given in N.

mean contact force, however, the largest variation in the standard deviation is to be found when the gradient returns to zero from an increasing wire height rather than when the gradient changes from zero to a decreasing wire height. From the force trace in Figure 9, this larger spread in data is a response to the sudden increase in contact force at locations 3 and 4 where the contact force prior to its increase was reduced due to the decreasing wire height at locations 1 and 2.

Varying contact wire and system heights

The results in the previous section were all obtained using model 2: keeping the dropper lengths the same in each span. While this is useful for investigating the effect of gradients, it is more realistic that the system heights are changed to make best use of the available space under low clearances. Taking the most extreme gradient considered in the previous section (1:100), two cases were considered:

Model 3: a reduction in wire and system heights
Model 4: a reduction in system height only.

For model 3, dropper lengths were calculated that would allow the catenary wire to drop down further than in model 2. The resulting geometries were given in Figures 5 and 6.

Table 7 shows a comparison between results from models 2, 3, and 4. The output shows no change in the overall behaviour with an increase of less than 0.1% in mean contact force between models 2 and 3 and no change between models 3 and 4. Reduced dynamic performance is predicted when reducing both the system and wire heights, represented by the 11% increase in standard deviation for model 4 compared with model 3. Maintaining the wire height and reducing the system height sees better performance results in a 24% reduction in standard deviation between models 2 and 4.

Figure 15 gives the force traces for each of the two interactions. Consistent with model 2, in Figure 15 a force peak is predicted by model 3 just before the support at 360 m. This results from the pantograph head accelerating due to the change from an ungraded wire to the decreasing 1:200 transition gradient. A force peak also occurs just after the last support at 780 m.

Whilst no gradients in the contact wire are imposed on model 4, the reduced system height and consequent change in stiffness yields a variation in the contact force. Figure 15

Table 7. Statistical output for models 2, 3 and 4.

Output	Model 2		Model 3	Model 4
	Level	1:100		
F_m	112	111	111	111
σ	11.5	18.0	19.9	13.6
$F_{D\,max}$	154	184	182	163
$F_{D\,min}$	90.2	75.4	57.2	79.4
$F_{S\,max}$	146	165	171	155
$F_{S\,min}$	77.4	57.3	51.6	73.6

Notes: Both level and graded contact wires are included for model 2. The wire gradient is maintained at 1:100 and data is taken over the whole working section and includes contributions from both falling and rising wire heights. All quantities given in N.

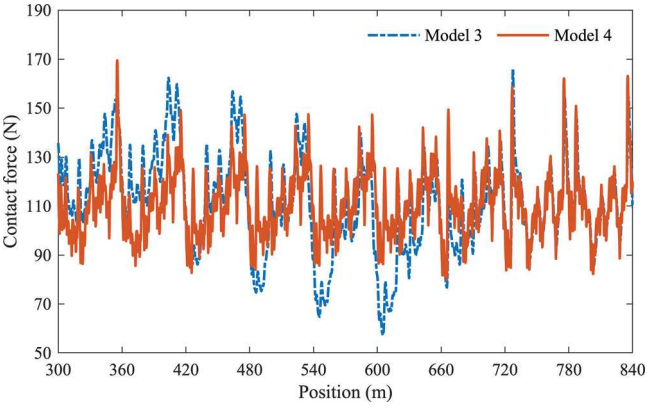

Figure 15. Contact force between the overhead line and pantograph head for models 3 and 4.

shows a predicted force peak at the support at 360 m. However, this force peak is more than 10% lower than those predicted in models 2 and 3 that include a reduction in the wire height. Beyond this force peak, from the force trace, an oscillatory behaviour in the force trace is predicted compared with models 2 and 3.

The trend of decreasing contact force from 480 m is consistent between models 2 and 3. Reducing the system height reduces the contact force further than in the constant system height case with the minimum contact force reduced by 24%. In contrast, the predicted peak contact force is almost unaffected by the introduction of reduced dropper lengths as only a 1% change is observed. This is thought to be due to the force peak occurring in the transition span when the dropper lengths are almost unchanged from model 2.

As with model 2, a moving window was used to analyse the mean contact force. The moving window average for a 1:100 gradient for all four models is given in Figure 16.

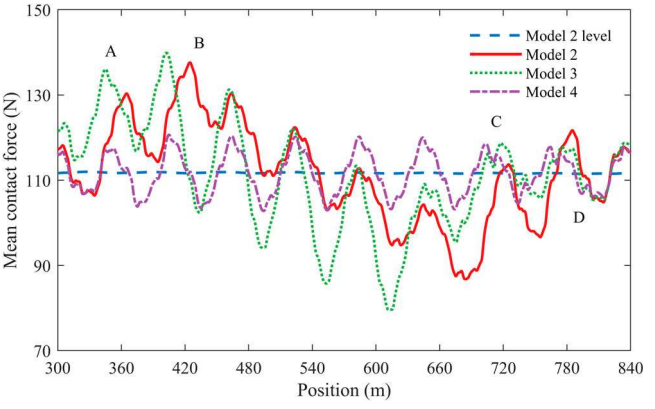

Figure 16. Mean contact force for models 2,3 and 4 using a 60 m window.

Compared with model 2, by reducing the length of the droppers, the mean contact force for model 3 is consistently lower between locations B and C indicated in Figure 16. When transitioning to a graded wire at location A, a 2.4% increase is predicted whilst transitioning to an ungraded wire at location D sees a 2.7% predicted decrease.

In all three models (2, 3, and 4), the saw-tooth pattern of higher contact force at mid-span was observed, however, reducing both the contact wire and system heights in model 3 yields a larger range (63 N) in the mean contact force when compared with models 2 (51 N) and 4 (20 N). In all three cases no contact loss was predicted.

Contact force response to train speed

The previous sections have focused on a train running speed of 200 km/h. To ensure the results are generalisable two further train speeds are considered, 130 and 225 km/h using model 2 with a contact wire gradient of 1:200. The statistical output is given in Table 8 and shows that the train speed is a dominant driver of the contact force, with a 9% increase in the mean force when the train speed is increased by 12.5%. The 54% increase in train speed from 130 to 200 km/h also yielded a 26% increase in the mean contact force. These are in line with the increase in mean contact forces given in [27]. Peak forces follow a similar trend, with 21% and 10% increases. These are larger than the increases observed when the gradient was increased to 1:100 but the train speed was maintained at 200 km/h suggesting that train speed is a significant force driver compared with the overhead line geometry.

Consequences and mitigations

Compared with 1:500 wire gradients, the peak contact force for 1:100 wire gradients is 14% higher. The increased contact force suggests these locations will experience greater wear, potentially shortening the lifetime of the OLE. Assuming that Archard's wear law [15] applies and the system remains within the mild wear regime, a 14% reduction in wire life would be expected for this worst-case gradient. Since no loss of contact between the pantograph head and contact wire is predicted for any of the studied height transitions,

arcing and any associated degradation of the OLE is not expected to increase. If this were carried through to a whole system life reduction of 14%, it may be acceptable against the alternative of an expensive bridge reconstruction, and for gradients shallower than 1:100 a far smaller decrease in life is predicted.

To mitigate the effect of increased peak forces, an overlap section could be installed under low clearance structures carrying a thicker contact wire, thus maintaining the current lifetime of the OLE. Three options are proposed for the length of contact wire throughout the height transition:

1. Install a thicker contact wire through the entire height transition section,
2. Install a second contact wire in locations where the peak contact forces occur. This, alongside the existing standard contact wire, would allow for force to be shared between them, or
3. Install contenary or a double contact wire, thereby eliminating the messenger wire and allowing for the installation of a thicker wire under the bridge.

All of the options would be a cost-saving compared with reconstructing a bridge. Which option is best would depend on the practicalities of sourcing, installing and maintaining a thicker contact wire compared with implementing the twin contact wire system. For each of the options, an increase in the effective mass of the contact wire will have an effect on the OLE dynamics; in particular, the increased contact mass could have a detrimental effect on the pantograph head at high speeds. Further modelling is required to assess the feasibility of these options alongside their costs.

Before steeper contact wires can be safely used on the network further analyses required would include checking:

- a further range of speeds below and above the 200 km/h considered here are not associated with high-force resonances,
- the effect of different designs of pantograph, in particular a further developed version of the existing HSX or a new pantograph that replicates the dynamic performance predicted by the modelling, and any anticipated degraded-mode running (e.g. if damping becomes less effective),
- the effect of multiple pantographs, particularly since the highest forces and most frequent losses of contact are associated with the trailing pantograph of a train running with more than one pantograph.

Table 8. Results for model 2 with a wire gradient of 1:200 for the train speeds considered.

Speed (km/h)	F_m	σ	$F_{D\max}$	$F_{D\min}$	$F_{S\max}$	$F_{S\min}$
130	89.2	10.3	141	74.5	120	58.3
200	112	14.7	170	80.1	156	67.5
225	122	18.3	187	64.1	177	67.1

Notes: Mean and standard deviation are taken over the entire working section. The data includes variation in the contact force due to both decreasing and increasing wire heights. All results are given in N.

Conclusions

Modelling has been undertaken to better understand the influence of wire gradients on the interaction between a pantograph and contact wire. Successful validation of a variable wire height model was undertaken; the model was in good agreement with the measured data in alignment with the standard.

The influence of contact wire gradients on the dynamic performance of the system has been investigated using both an idealised system with constant dropper lengths and systems with altered dropper lengths, better representing more realistic OLE installations. The contact wire gradient was increased up to 1:100, far exceeding the current allowable gradients. Results show that exceeding the standard maximum gradient of 1:500 leads to only a 14% increase in the peak force even when the gradient is increased to 1:100. Overall system life is driven by a complex combination of fatigue, mechanical and electrical wear, but taking mechanical wear alone the effect on wire life is indicated by the Archard wear law. Assuming a mild wear regime, a 14% increase in load would lead to a 14% reduction in mechanical wear life, for a 1:200 gradient, the indication would be a 5.6% reduction.

Considering averages over the 60 m length of each span, the range of mean contact force was found to increase for steeper gradients. The range between the maximum and minimum of the mean contact force was 32 N for a maximum wire gradient of 1:100 compared with a range of 11 N for a wire gradient of 1:500.

Overall, the primary outcome of this high-level study of the catenary pantograph interaction, is that the validated model has indicated that using steeper wire gradients to avoid reconstructing bridges is unlikely to cause any significant problems on the rail system and may represent significant cost benefits to infrastructure owners. To mitigate the effects of the increased contact force, three methods of mitigation have been proposed which would be expected to have costs significantly lower than reconstruction of infrastructure to accommodate shallow wire gradients. Further work is proposed to assess the feasibility of these methods discussed in terms of effect on the dynamics of the system as well as the cost implications. Whilst in this study the focus has been on a single pantograph and three separate running speeds, further work is also recommended to investigate the influence of wire gradients on multiple pantograph operation and different train running speeds aligning with resonances of the equipment. It is also proposed that testing of the contact wire is undertaken to determine the transition from mild to severe wear.

Acknowledgements

The authors would like to acknowledge data provided by Furrer + Frey and Patric Mak of Network Rail as well as Chris Bryan for fruitful discussions and support throughout the project.

Disclosure statement

No potential conflict of interest was reported by the author(s).

Funding

The authors gratefully acknowledge financial support provided by the Engineering and Physical Sciences Research Council [grant number 1802703] and Furrer + Frey for this work.

ORCID

Sam Hayes http://orcid.org/0000-0002-2831-5413

References

[1] Network Rail. Route utilisation strategy, electrification. London: Network Rail; 2009.
[2] Bruni S, Bucca G, Carnevale M, et al. Pantograph–catenary interaction: recent achievements and future research challenges. Int J Rail Transp. 2018;6(2):57–82. doi: 10.1080/23248378.2017.1400156.
[3] Kia SH, Bartolini F, Mpanda-Mabwe A, et al. Pantograph-catenary interaction model comparison. In IECON 2010-36th Annual Conference on IEEE Industrial Electronics Society; 2010 pp. 1584–1589.
[4] Song D, Jiang Y, Zhang W. Dynamic performance of a pantograph–catenary system with consideration of the contact surface. Proceedings of the Institution of Mechanical Engineers, Part F: Journal of Rail and Rapid Transit. 2018;232(1):262–274.
[5] BSI. BS EN 50119:2009+A1:2013: railway applications. Fixed installations. Electric traction overhead contact lines. London: BSI; 2009.
[6] RSSB. Railway Group standard GLRT1210 AC energy subsystem and interfaces to rolling stock subsystem. London: RSSB; 2019.
[7] Williams J. Engineering tribology. Oxford: Oxford University Press; 1994.
[8] Bucca G, Collina A. A procedure for the wear prediction of collector strip and contact wire in pantograph–catenary system. Wear. 2009;266(1–2):46–59. doi:10.1016/J.WEAR.2008.05.006.
[9] Gonzalez FJ, Chover JA, Suarez B, et al. Dynamic analysis using finite elements to calculate the critical wear section of the contact wire in suburban railway overhead conductor rails. Proc Inst Mech Eng Part F J Rail Rapid Transit. 2008;222(2):145–157. doi:10.1243/09544097JRRT144.
[10] Kubo S, Kato K. Effect of arc discharge on wear rate of Cu-impregnated carbon strip in unlubricated sliding against Cu trolley under electric current. Wear. 1998;216(2):172–178. doi:10.1016/S0043-1648(97)00184-1.
[11] Ambrósio J, Pombo J, Pereira M, et al. A computational procedure for the dynamic analysis of the catenary-pantograph interaction in high-speed trains. J Theor Appl Mech. 2012;50(3):681–699.
[12] Seo J-H, et al. Dynamic analysis of a pantograph–catenary system using absolute nodal coordinates. Veh Syst Dyn Aug. 2006;44(8):615–630. doi:10.1080/00423110500373721.
[13] Vo Van O, Massat J-P, Balmes E. Waves, modes and properties with a major impact on dynamic pantograph-catenary interaction. J Sound Vib 2017;402:51–69. doi:http://doi.org/10.1016/j.jsv.2017.05.008.
[14] Antunes P, Ambrósio J, Pombo J, et al. A new methodology to study the pantograph–catenary dynamics in curved railway tracks. Veh Syst Dyn Mar. 2020;58(3):425–452. doi:10.1080/00423114.2019.1583348.
[15] BSI. BS EN 50318:2002: railway applications - current collection systems - requirements for and validation of measurements of the dynamic interaction between pantograph and overhead contact line. London: BSI British Standards; 2002.
[16] Bruni S, et al. The results of the pantograph–catenary interaction benchmark. Veh Syst Dyn 2015;53(3):412–435. doi:10.1080/00423114.2014.953183.
[17] Nåvik P, Rønnquist A. Dynamic behaviour of an existing railway catenary system for extreme low passage at exceeding design velocities. In Proceedings of the 9th International Conference on Structural Dynamics, 2014, no. July, pp. 3753–3760.

[18] Beagles A, Fletcher D, Peffers M, et al. Validation of a new model for railway overhead line dynamics. Proc ICE-Transport. 2016;169(5):339–349.
[19] Bryan C. Overhead line dynamic performance – using statistical design to aid computer simulation of series 1 equipment. Milton Keynes: Network Rail; 2014.
[20] Bryan C. Series 1 Old Dalby test results – data processing summary of Brecknell Willis pantograph tests. Milton Keynes: Network Rail; 2014.
[21] Conway S. Lump mass models for legacy pantographs on GB mainline. London: RSSB; 2016.
[22] Vyasarayani CP, Uchida T, Carvalho A, et al. Parameter identification in dynamic systems using the homotopy optimization approach. Multibody Syst Dyn. 2011;26(4):411–424. doi:10.1007/s11044-011-9260-0.
[23] BSI. BS EN 50206 – 1:2010 railway applications – Rolling stock – pantographs: characteristics and tests part 1: pantographs for main line vehicles. London: BSI British Standards; 2010.
[24] BSI. BS EN 50317:2012 railway applications. current collection systems. Requirements for and validation of measurements of the dynamic interaction between pantograph and overhead contact line. London: BSI Britsh Standards; 2012.
[25] Navik P, Ronnquist A, Stichel S. Variation in predicting pantograph-catenary interaction contact forces, numerical simulations and field measurements. Veh Syst Dyn. 2017;55(9):1265–1282.
[26] Blevins RD. Formulas for dynamics, acoustics and vibration. Oxford: Wiley-Blackwell; 2015.
[27] BSI. BS EN 50367:2012+A1:2016 railway applications. current collection systems. Technical criteria for the interaction between pantograph and overhead line (to achieve free access). London: BSI British Standards; 2012.